# Factors responsible for the stability and the existence of a clean energy gap of a silicon nanocluster

Lei Liu, C. S. Jayanthi, and Shi-Yu Wu[a)]
*Department of Physics, University of Louisville, Louisville, Kentucky 40292*

(Received 30 March 2001; accepted for publication 18 July 2001)

We present a critical theoretical study of electronic properties of silicon nanoclusters, in particular the roles played by symmetry, relaxation, and hydrogen passivation on the stability, the gap states and the energy gap of the system using the order N [O(N)] nonorthogonal tight-binding molecular dynamics and the local analysis of electronic structure. We find that for an unrelaxed cluster with its atoms occupying the regular tetrahedral network, the presence of undistorted local bonding configuration is sufficient for the appearance of a small clean energy gap. However, the energy gap of the unrelaxed cluster does not start at the highest occupied molecular orbital (HOMO). In fact, between the HOMO and the lower edge of the energy gap, localized dangling bond states are found. With hydrogen passivation, the localized dangling bond states are eliminated, resulting in a wider and clean energy gap. Relaxation of these hydrogen passivated clusters does not alter either the structure or the energy gap appreciably. However, if the silicon clusters are allowed to relax first, the majority of the dangling bonds are eliminated but additional defect states due to bond distortion appear, making the energy gap dirty. Hydrogen passivation of these relaxed clusters will further eliminate most of the remnant dangling bonds but no appreciable effect on the defect states associated with bond distortions will take place, thus still resulting in a dirty gap. For the hydrogen-passivated $Si_N$ nanoclusters with no bond distortion and no overall symmetry, we have studied the variation of the energy gap as a function of size of the cluster for $N$ in the range of $80<N<6000$. The dependence of the energy gap on the size shows similar behavior to that for silicon nanoclusters with no bond distortion but possessing overall symmetry.  [DOI: 10.1063/1.1402672]

## I. INTRODUCTION

The discovery of photoluminescence (PL) in the visible regime[1] from porous silicon has prompted many experimental[2–5] and theoretical investigations,[6–12] both because of the implications of this phenomenon in the fabrication of silicon-based optoelectronic devices and the interest in understanding this phenomenon. The intensive research following this discovery seemed to suggest that strong optical transitions can be expected only from those Si-based systems which have an effective reduced dimensionality. Structural studies of porous Si showed that porous Si is composed of Si nanostructures in the forms of columns and clusters.[3,4,13] Hence, the ensuing research efforts have placed emphasis on the electronic and optical properties of silicon nanoclusters. Two mechanisms have been proposed to explain the observation of enhanced PL. The first suggests that the strong PL in the visible regime is due to the enhancement of the momentum matrix elements associated with the confinement of the electronic wave functions[14–17] of silicon nanoparticles. The second suggests that the surface chemical composition of silicon nanostructures may also play a key role in the enhanced PL.[18–20] Most recently, experimental evidence[21] seemed to suggest the blue emission from silicon nanoparticles of 1 nm in diameter that was attributed to the photoexcitation of Si–Si surface states.[22,23] In all these mechanisms, the existence of a clean energy gap plays a pivotal role in determining the efficiency of the luminescence. Furthermore, since the PL for the bulk crystalline silicon is in the near infrared regime while it is in the visible regime for silicon nanoparticles, a great deal of effort has been devoted to the study of size dependence of the gap of Si nanoparticles.[6–12]

In the present work, we focus on issues that are relevant to the fabrication of device-quality silicon nanostructures. We aim to obtain a clear understanding of the physics governing the existence of a clean energy gap in silicon nanoclusters by studying the role played by hydrogen passivation, relaxation, and symmetry. Previous theoretical studies, particularly those pertaining to the size dependence of the energy gap, focused on a highly symmetric configuration where the surface dangling bonds are completely passivated by hydrogen atoms so that the system possesses the regular tetrahedral bonding configuration as well as an overall symmetry. But it is difficult experimentally to control the number of atoms in a silicon nanocluster. Hence, in most cases, the experimentally fabricated samples of silicon nanoclusters will not possess an overall symmetry. Therefore there are two issues that need to be resolved for such general clusters. The first issue is related to the question: ''Can a general cluster without an overall symmetry exhibit a wide and clean gap?'' The other issue is related to the size dependence of the gap of a general cluster. In this work, we will compare the

a)Author to whom correspondence should be addressed; electronic mail: sywu0001@fellini.physics.louisville.edu

 

results for nanoclusters with an overall symmetry to those with no overall symmetry. We will consider both hydrogen-passivated clusters and those with no hydrogen passivation. Finally, we will consider both unrelaxed and relaxed nanoclusters. More specifically, we will address the following issues: (i) How do we obtain a clean energy gap in the case of silicon nanoclusters? (ii) What is the nature of the gap states? (iii) What is the role of relaxation and hydrogen passivation on the energy gap and gap states? (iv) Is there an intrinsic relationship between the energy gap and the local bonding configuration? (v) How is a nanocluster with full symmetry different from a cluster with no overall symmetry with regard to the existence of a clean gap?

In this work we have used a combination of theoretical studies to investigate the structure, the stability, the energy gap, and the electronic density of states (EDOS) of the nanocluster. We use the nonorthogonal tight-binding (NOTB) molecular dynamics[24] to determine the structure of silicon nanoclusters. For sizes of the cluster with $n>500$, we have used the order N [O(N)] technique, as developed in Ref. 25, to determine the equilibrium structure. Similarly, to circumvent the difficulties associated with an accurate calculation of the energy gap of a large cluster, we have devised a method, as described in the Appendix of this article, that directly computes the eigenvalues corresponding to the highest occupied molecular orbital (HOMO) and the lowest unoccupied molecular orbital (LUMO) without having to obtain the entire eigenvalue spectrum. Finally, the electronic density of states is calculated using the real-space Green's function (RSGF) technique as developed in Ref. 26.

This article is organized as follows. In Sec. II, we consider Si nanoclusters with no overall tetrahedral symmetry (e.g., $Si_{200}$, $Si_{800}$, and $Si_{2000}$) and illustrate how the relaxation of such systems, while leading to the stability of the system, precludes the formation of a clean energy gap. In Sec. III, we consider a silicon nanocluster with overall tetrahedral symmetry (e.g., $Si_{83}$) and investigate in detail the role of hydrogen passivation on the stability, the energy gap, and gap states of such a cluster. In Sec. IV, we consider the hydrogen passivation of clusters with no overall tetrahedral symmetry and compare our results with the case discussed in Sec. III. In Sec. V, the variation of the energy gap as a function of the size of the hydrogen-passivated nanocluster with no overall symmetry is given. Finally, in the Appendix, we present the formalism used in this article for the calculation of HOMO and LUMO energies of a large cluster.

## II. INTERPLAY BETWEEN RELAXATION, STABILITY, AND ENERGY GAP

A nanocluster, left to itself, will search for a stable configuration by relaxation and "surface" reconstruction. The process is triggered by the tendency of a cluster to minimize its total energy with the elimination of the dangling bonds associated with the exterior atoms. But it often comes at a price as it causes severe distortion of the bonds, in particular of the exterior atoms.[27] As a result, defect states associated with bond distortions are expected to appear. Furthermore, relaxation may not completely eliminate the dangling bonds on the surface. Hence there will also be defect states associated with remnant dangling bonds. Both these defect states may fall in the gap region, making the gap less clean or even "dirty."

TABLE I. NOTB parameters for silicon–silicon and silicon–hydrogen interactions are given. The orbital energies used in the calculation are $\varepsilon_s(\mathrm{Si}) = -13.55$ eV, $\varepsilon_p(\mathrm{Si}) = -6.52$ eV, and $\varepsilon_s(\mathrm{H}) = -8.67$ eV. The parameters characterizing the NOTB Hamiltonian and the notations are described in Ref. 24.

| | $d_0$(Å) | $\alpha$(Å$^{-1}$) | $K_0$ | $\chi_0$(eV) | $\sigma$(Å$^{-2}$) |
|---|---|---|---|---|---|
| Si–Si | 2.36 | 1.62 | 1.7 | 0.41 | 2.5 |
| Si–H | 1.71 | 1.76 | 1.7 | 0.41 | 2.5 |

To verify the validity of this picture, we have performed the full-geometry optimization of Si nanoclusters of different sizes using the O(N)–NOTB–molecular dynamics (MD) and then determined their EDOS. The NOTB Hamiltonian for silicon used in this work is that of Menon and Subbaswamy.[24] The parameters characterizing this Hamiltonian are summarized in Table I. This Hamiltonian has been used in the literature and is known to yield reliable structure for the bulk Si (diamond phase),[24] Si clusters,[24,28] and Si(100) surface ($c4\times2$ reconstruction).[29] In this section, we first consider those silicon clusters whose atoms when arranged in a regular tetrahedral network do not form a complete shell. We have deliberately chosen to study this system as we are interested in comparing the energy gap results for clusters not possessing overall tetrahedral symmetry (e.g., $Si_{200}$, $Si_{800}$, and $Si_{2000}$) with those having this symmetry (e.g., $Si_{83}$). The results of the latter case will be reported in Sec. III.

In our simulations, a stable configuration for a cluster of a given size is considered to have been reached if the magnitude of the force acting on each atom is on the order of $10^{-2}$ eV/Å and the total energy of the configuration is a minimum. Figure 1 shows the optimized structure for $Si_{2000}$. It can be seen that the interior of the cluster has the bulk-like tetrahedral structure. On the "surface" of this cluster, fea-

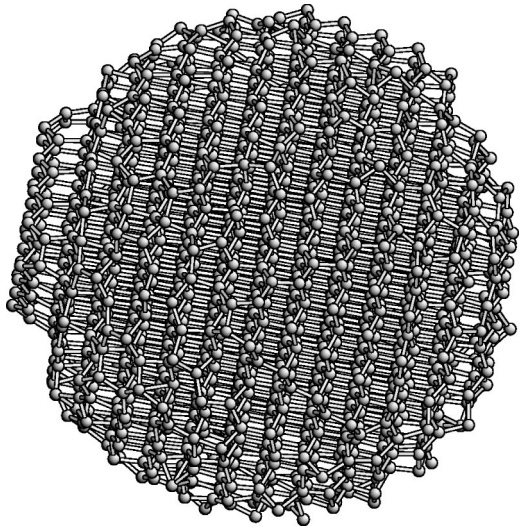

FIG. 1. Optimized structure of $Si_{2000}$ as obtained by the O(N)/NOTB-MD method.

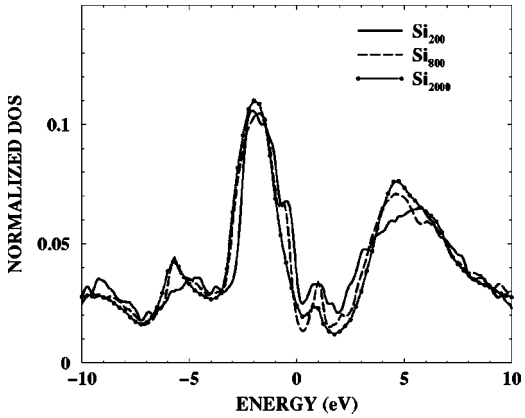


FIG. 2. A comparison of the normalized electronic density of states of relaxed $Si_{200}$, $Si_{800}$ and $Si_{2000}$, respectively. No discernible gap is seen in this case, where the energy of HOMO level is fixed at zero.

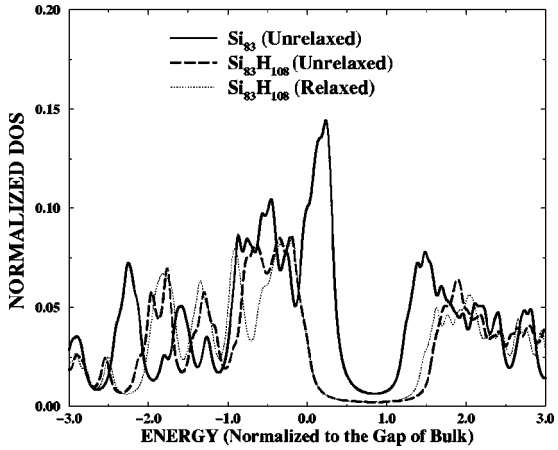


FIG. 3. A comparison of the normalized electronic density of states of the unrelaxed $Si_{83}$ unrelaxed $Si_{83}H_{108}$, and relaxed $Si_{83}H_{108}$, respectively. The energy of HOMO for each case is set at zero.

tures resembling the adatoms in the $Si(111)7\times7$ reconstruction,[30] and dimer rows associated with $Si(100)$[29] have emerged. The general features of the other clusters studied are similar to those characterizing the $Si_{2000}$ cluster, namely, the bonding configurations of the interior atoms are bulk-like and the surface features exhibit the characteristics of the most stable surface reconstruction of Si.[25] However, the bonding configurations of exterior atoms show more severe distortions from the regular tetrahedral network as the size of the cluster decreases.

A survey of the exterior atoms in these clusters (see Fig. 1) shows that most of them are three-fold bonded. Thus, most of the dangling bonds associated with the unrelaxed exterior atoms have been eliminated by the surface reconstruction, specifically the tendency of the Si atoms on the surface to dimerize or the capping of the dangling bonds by adatoms. From Fig. 1, it can be seen that, as a result of reconstruction such as dimerization or capping, the bonding configurations associated with the exterior atoms are distorted from the regular tetrahedral network, some more so than others.

In Fig. 2, the EDOS of the stable configuration of $Si_N$ clusters for $N=200$, 800, and 2000 are shown, where the energy of the HOMO for each case is taken to be zero. A key feature, which stands out in all three plots of density of states, is that there is no well-defined energy gap above the HOMO ($E=0$) in the band gap region of a semiconducting Si system. Instead, defect states due to the remnant dangling bonds and distorted bonding configurations are found in the gap region. This calculation demonstrates that the disappearance of a clean gap is the price for achieving the stability of a Si nanocluster on its own. In other words, a ''pure'' and stable Si nanocluster will not have a well-defined gap that is comparable to the gap of a bulk Si.

## III. ROLE OF HYDROGEN PASSIVATION ON THE STABILITY AND THE EXISTENCE OF A CLEAN GAP FOR A CLUSTER WITH COMPLETE SHELL

Previous theoretical studies on hydrogen-passivated *unrelaxed* Si clusters with an overall symmetry and no local bond distortion have shown the existence of a clean and well-defined energy gap and that the gap is blueshifted as the size of the nanocluster is reduced.[6] However, the role of hydrogen passivation in eliminating the defect states has not been analyzed thoroughly in these studies. Also, a detailed analysis of the stability of these structures has not been provided.

To shed light on these issues, we consider a $Si_{83}$ cluster whose atoms occupy complete shells of a regular bulk tetrahedral network so that the cluster not only possesses local tetrahedral bonding configuration but also an overall symmetry. The reason for choosing a small-sized cluster is that it is more convenient to analyze its properties in terms of hydrogen passivation while the underlying physics concerning hydrogen passivation is basically the same regardless of the size of the system. In the following, we will investigate the role played by hydrogen passivation in eliminating the dangling bonds and stabilizing the system for both unrelaxed and relaxed clusters. In considering relaxed clusters, we will make a further distinction between the case when the silicon cluster is first passivated and then relaxed and the one in which the cluster is first relaxed and then passivated.

We start by calculating the EDOS of the *unrelaxed* $Si_{83}$ cluster whose structure is identical to the bulk structure, including the bond length (as determined by Menon and Subbaswamy's NOTB Hamiltonian).[24] For the unrelaxed $Si_{83}$ cluster, each of the 41 interior atoms has four bonds both by the simple distance criterion as well as by the bond charge criterion,[28] while the remaining 42 exterior atoms have in total 108 dangling bonds. Clearly, $Si_{83}$ with 108 dangling bonds is not a stable structure. The DOS for this structure is meant only to serve as a benchmark for comparisons with other cases. The result of this calculation, together with the density of states corresponding to the cases of unrelaxed $Si_{83}H_{108}$ and relaxed $Si_{83}H_{108}$ clusters, respectively, are shown in Fig. 3. The unrelaxed structure of $Si_{83}H_{108}$ is obtained by attaching a hydrogen atom for each dangling bond along the tetrahedral bonding direction. For the hydrogen passivated Si clusters, the parameters characterizing the Si–H interactions within the NOTB formulation were obtained by fitting to the bond length of Si–H and the molecu-

lar orbital energy of $SiH_4$.[31,32] The relevant parameters of this interaction are also listed in Table I. It should be noted that the DOS plots in this and subsequent figures are always displayed with the energy of HOMO for each case set to zero.

A cursory examination of the DOS plots shown in Fig. 3 reveals the following points: (1) There is a well-defined and substantial clean gap for the DOS corresponding to the unrelaxed (unstable) $Si_{83}$ cluster. But this gap does not begin at the energy of HOMO ($E=0$). There are two prominent peaks at the two extremities of the gap. The first peak is immediately above the HOMO ($E=0$) while the second peak is above the gap. Comparing the appearance of a well-defined gap in the DOS of this unrelaxed $Si_{83}$ with no gap for relaxed clusters discussed in Sec. II, one can easily associate the existence of a clean gap either with the local bonding configuration and/or the overall symmetry of the cluster. (2) With the passivation of the 108 dangling bonds associated with the exterior atoms, the gap of the unrelaxed $Si_{83}H_{108}$ cluster ''opens'' up substantially with respect to the gap of the unrelaxed $Si_{83}$. This gap now begins at the energy of HOMO. A comparison of these two density of states leads to an impression that the ''opening'' of the gap in $Si_{83}H_{108}$ has resulted from the elimination of the two broad peaks in the DOS of the unrelaxed $Si_{83}$, one immediately above the energy of HOMO of $Si_{83}$ and the other across the gap from the first peak. Since there is no distortion in the bonding configurations of the exterior atoms in the unrelaxed $Si_{83}$, the defect states are entirely due to the 108 dangling bonds. One can then conclude that the opening up of the gap is due to the saturation of the dangling bonds by hydrogen passivation. Furthermore, one might even be tempted to attribute the two broad peaks as being associated with the dangling bond states. (3) After we relaxed the hydrogen passivated $Si_{83}H_{108}$ cluster, we find that there is hardly any change in the major part of the gap region of the relaxed $Si_{83}H_{108}$ as compared to that of the unrelaxed $Si_{83}H_{108}$, with only a slight narrowing of the gap due to a small downward shift of the energy of LUMO. The main features of the density of states of the two cases (unrelaxed and relaxed $Si_{83}H_{108}$) are also very similar. There is, however, some modification in the interior of the bands with the appearance of features which can be identified with Si–H bonding (see the discussion following Figs. 7 and 8, respectively).

To build a complete understanding of the effects of passivation, we have carried out a local analysis of the electronic structure of the unrelaxed $Si_{83}$ as well as the unrelaxed $Si_{83}H_{108}$ clusters. In the framework of a NOTB approach, the electronic structure is determined by solving a general eigenvalue problem

$$HC_\lambda = E_\lambda S C_\lambda, \tag{1}$$

where $C_\lambda$ is the column vector representing the coefficients of expansion of the wave function $\Psi_\lambda$ with the eigenenergy $E_\lambda$ in terms of some localized basis set $\phi_{i\alpha}$ not explicitly stated. Here $i$ refers to the atomic site and $\alpha$ the orbitals at site $i$. The Hamiltonian matrix elements $H$ and the overlapping matrix elements $S$ are defined as

$$H_{i\alpha,j\beta} = \int \phi_{i\alpha}(\mathbf{r}) \mathcal{H} \phi_{j\beta}(\mathbf{r}) d\mathbf{r}, \tag{2}$$

$$S_{i\alpha,j\beta} = \int \phi_{i\alpha}(\mathbf{r}) \phi_{j\beta}(\mathbf{r}) d\mathbf{r}. \tag{3}$$

But in the semiempirical NOTB approach, these matrix elements are treated as parameterized functions of $\mathbf{R}_{ij}=\mathbf{R}_j-\mathbf{R}_i$ with the relevant parameters fitted to experimental results and/or first principles calculations. The details of the NOTB formulation can be found in Ref. 24.

Within the framework of the NOTB treatment, the electronic DOS can be expressed as[25,28]

$$\rho(E) = \sum_{\lambda,i\alpha,j\beta} c_{i\alpha,\lambda} c_{j\beta,\lambda} S_{j\beta,i\alpha} \delta(E-E_\lambda)$$

$$= \lim_{\epsilon\to 0} \frac{1}{\pi} \sum_{\lambda,i\alpha,j\beta} c_{i\alpha} c_{j\beta} S_{i\alpha,j\beta} \frac{\epsilon}{(E-E_\lambda)^2+\epsilon^2}. \tag{4}$$

Equation (4) allows one to rewrite the DOS in terms of the local DOS (LDOS) $\rho_i(E)$ such that

$$\rho(E) = \sum_i \rho_i(E) \tag{5}$$

with

$$\rho_i(E) = \sum_{\lambda,\alpha,j\beta} c_{i\alpha} c_{j\beta} S_{j\beta,i\alpha} \delta(E-E_\lambda). \tag{6}$$

The NOTB Hamiltonian used in this study was developed in a $sp^3$ framework. For the unrelaxed $Si_{83}$ cluster, there are then $83\times 4=332$ possible states. Subtracting the 108 dangling bond states, there are 224 states with half of them (112) being the bonding states and the other half antibonding states. In the meantime, there are 332 valence electrons in $Si_{83}$ and they occupy the lowest 166 states. Out of these 166 states, 112 are the bonding states. This means that the remaining $166-112=54$ states must come from the 108 dangling bond states, leaving the other 54 dangling bond states unoccupied. To understand the characteristics of these states, we define a quantity

$$A_i(E_{\lambda_1},E_{\lambda_2}) = \int_{E_{\lambda_1}^-}^{E_{\lambda_2}^+} \rho_i(E) dE, \tag{7}$$

where $E_{\lambda_1}^- = E_{\lambda_1} - 0^+$ and $E_{\lambda_2}^+ = E_{\lambda_2} + 0^+$. This quantity is the local contributions to the integrated DOS for the eigenstates in the energy interval $[E_{\lambda_1}, E_{\lambda_2}]$. Hence this quantity will be referred to as the partially integrated LDOS (PILDOS). When PILDOS is plotted against the site index $i$, it provides a transparent picture as to whether states in a certain energy interval are extended throughout the cluster or only restricted in a certain region of the cluster. (In this work, atoms are labeled from inside to outside.) In Fig. 4, $A_i$ for the following energy intervals are shown, namely, $A_i(E_1,E_{112})$, $A_i(E_{113},E_{166})$, and $A_i(E_{167},E_{220})$. It can be seen that the $A_i$ for the first 112 states, i.e., $A_i(E_1,E_{112})$ is almost uniformly distributed throughout the 83 sites of the unrelaxed $Si_{83}$ cluster. Hence the first 112 states must be the 112 extended bonding states. The $A_i$ corresponding to the next 54 states,

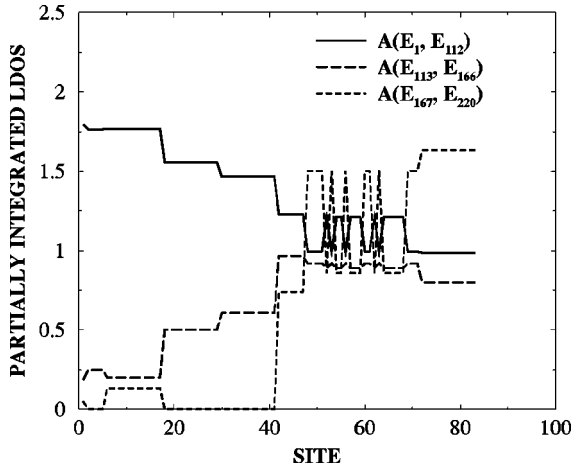


FIG. 4. Partially integrated local density of states is plotted for three different energy intervals (two below and one above the HOMO level) at the sites of the unrelaxed $Si_{83}$ cluster.

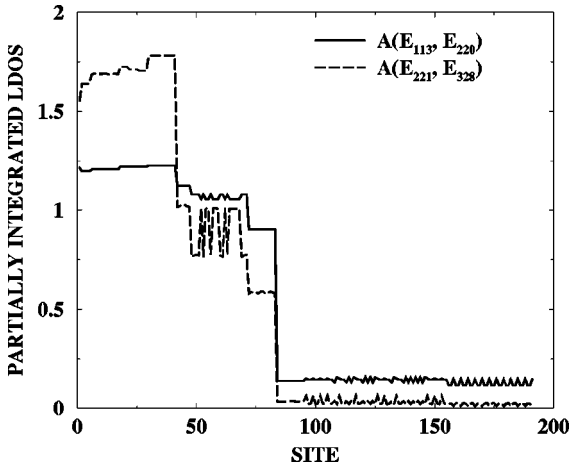


FIG. 6. Partially integrated local density of states is plotted at the sites of unrelaxed $Si_{83}H_{108}$ cluster.

$A_i(E_{113},E_{166})$, is mostly concentrated in the region of the 42 exterior sites, indicating that these 54 states (113–166) must be the occupied dangling bond states. The $A_i$ for the 54 states from 167 to 220 is almost entirely localized in the surface region of the 42 exterior sites. Hence these 54 states must correspond to the 54 unoccupied dangling bond states. In Fig. 5, the $A_i$s for the 54 states from 221 to 274 are shown in three subintervals of 18 states each, namely, $A_i(E_{221},E_{238})$, $A_i(E_{239},E_{256})$, and $A_i(E_{257},E_{274})$. It can be seen that these $A_i$ are distributed throughout the 83 sites of the cluster, indicating that these 54 states must be the extended antibonding states. Thus the first broad peak in the DOS of the unrelaxed $Si_{83}$ just above the energy of HOMO (seen in Fig. 3) which covers the energy range from $E_{167}$ to $E_{220}$ is indeed composed of the dangling bond states (unoccupied) while the second broad peak above the gap, covering the energy range from $E_{221}$ to $E_{274}$, is composed entirely of extended antibonding states. In this regard, this second broad peak above the gap in the DOS of the unrelaxed $Si_{83}$ cluster can be attributed to the downward shift (in energy) of the extended antibonding states due to the presence of the dangling bond states.

For the unrelaxed $Si_{83}H_{108}$ where the 108 dangling bonds of $Si_{83}$ are saturated by the 108 hydrogen atoms, there are altogether $83\times4+108\times1=440$ states with the 220 lowest states being the bonding states and the remaining 220 states the antibonding states. There are also 440 electrons in this cluster. Hence the 220 bonding states are completely occupied while the 220 antibonding states are unoccupied. The bonding and antibonding states are separated by a wide band gap. The picture presented above can be understood in terms of the $A_i$s for the unrelaxed $Si_{83}H_{108}$ shown in Fig. 6 where $A_i(E_{113},E_{220})$ and $A_i(E_{221},E_{328})$ are plotted. It can be seen that both $A_i$s are distributed uniformly throughout the 83 Si sites of the cluster with only very minor contributions from the outer 108 hydrogen sites, indicating that (i) these states are extended throughout the Si cluster and (ii) the widening of the gap is due to elimination of the localized dangling bond states. In Figs. 7 and 8, the LDOSs at two typical hydrogen sites corresponding to the elimination of two dangling bonds of a Si atom and those at three typical hydrogen

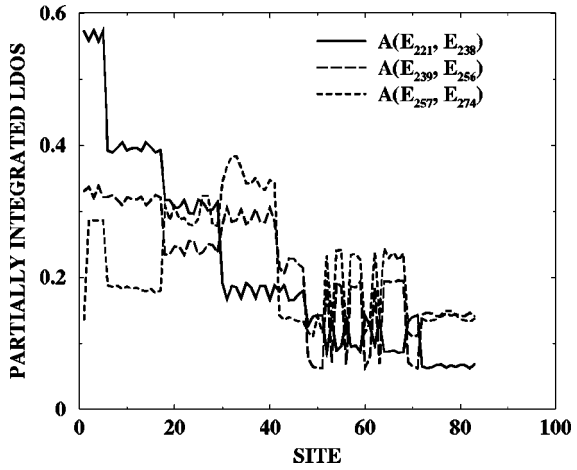


FIG. 5. Partially integrated local density of states is plotted at the sites of the unrelaxed $Si_{83}$ cluster for energy eigenvalue index 221–274 in steps of 18.

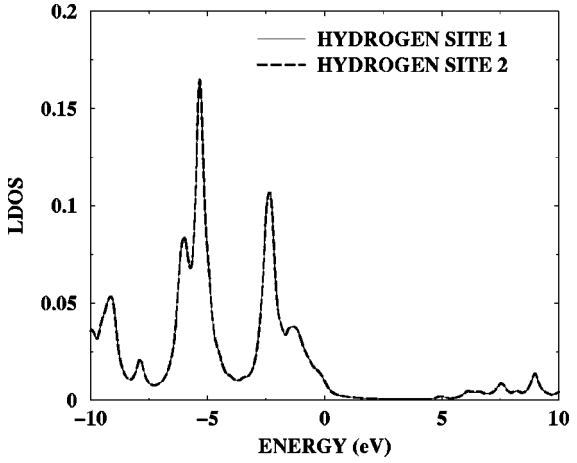


FIG. 7. Local density of states at hydrogen sites which typically saturate two dangling bonds associated with an exterior Si atom.

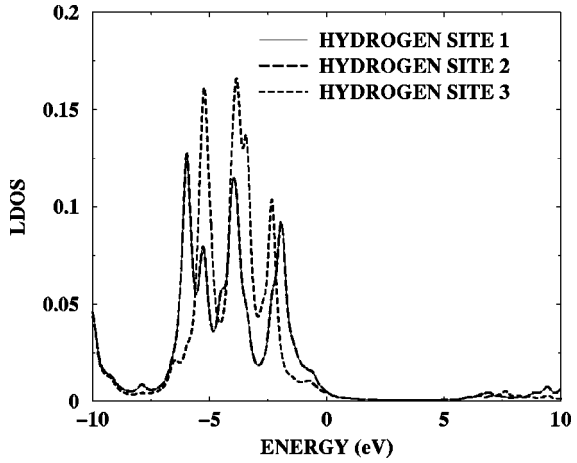


FIG. 8. Local density of states at hydrogen sites which typically saturate three dangling bonds associated with an exterior Si atom.

sites corresponding to elimination of three dangling bonds of a Si atom are shown, respectively. It can be seen that there is absolutely no contribution from the hydrogen site to the band edge states of the DOS of the unrelaxed $Si_{83}H_{108}$ cluster. The combined picture of Figs. 6, 7, and 8 shows convincingly that the existence of the clean band gap in the DOS of the unrelaxed $Si_{83}H_{108}$ is entirely due to the Si atoms in the cluster with no contribution from the surface chemistry of Si–H bonding. In other words, the role of hydrogen is simply to eliminate the dangling bonds at the surface of Si atoms.

We have also carried out the relaxation of $Si_{83}$ cluster to obtain a stable $Si_{83}$ structure. The relaxation process indeed eliminated many of the 108 dangling bonds associated with the unrelaxed $Si_{83}$. But this occurs at the expense of introducing severe bond distortion for the ''surface'' atoms, resulting in the appearance of bond distorted defect states in the gap (see Fig. 9). The coexistence of the distorted bond states and the remnant dangling bond states that are not eliminated by relaxation provides the explanation why Si nanoparticles deposited onto a film and aged in vacuum show no PL.[33] The relaxed stable $Si_{83}$ structure ($Si^r_{83}$) has only 22 dangling bonds. We then saturated these 22 dangling

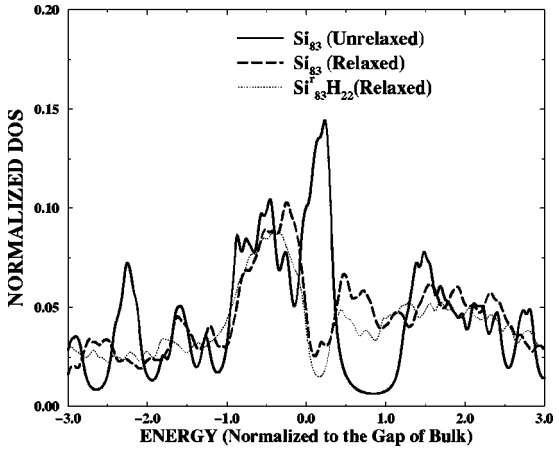


FIG. 9. A comparison of the normalized electronic density of states of unrelaxed $Si_{83}$, relaxed $Si_{83}$, and relaxed $Si_{83}H_{22}$ whose remnant dangling bonds are saturated with hydrogen atoms, respectively.

TABLE II. A comparison of the total energy for the various cases of $Si_{83}$ clusters studied in this work.

| $Si_{83}$ | | $Si_{83}H_{108}$ | | $Si^r_{83}H_{22}$ |
|---|---|---|---|---|
| Unrelaxed | Relaxed | Unrelaxed | Relaxed | Relaxed |
| −3724 eV | −3785 eV | −5419 eV | −5429 eV | −4113 eV |

bonds by hydrogen and relaxed the $Si^r_{83}H_{22}$ configuration. In Fig. 9, the density of states corresponding to unrelaxed $Si_{83}$, relaxed $Si_{83}$, and relaxed $Si^r_{83}H_{22}$ clusters are shown. It can be seen that the relaxation of $Si_{83}$ eliminated the majority of the dangling bonds and the passivation by hydrogen after the relaxation further reduced the remaining dangling bonds. But the distorted bonding configurations resulting from the surface reconstruction are mostly still present even for relaxed $Si^r_{83}H_{22}$. Hence hydrogen passivation of relaxed cluster is not expected to yield the best clean gap.

Finally, in Table II, we listed the comparison of the total energy for all the cases considered. It can be seen that the relaxed $Si_{83}H_{108}$ has the lowest energy (−5429 eV) while the unrelaxed $Si_{83}H_{108}$ has almost the same energy (−5419 eV). The two structures are also very similar, indicating that hydrogen passivation before the cluster has the time to relax is the best way to fabricate stable clusters with a clean gap.

## IV. HYDROGEN PASSIVATION OF CLUSTERS WITH INCOMPLETE SHELL

As pointed out in Sec. I, it is very difficult to control experimentally the number of atoms in a cluster. This simply means that, in the fabrication process, there is no way to be certain that the cluster will have exactly the desired number of atoms to complete the shell of, say, a tetrahedral network. The question must then be raised as to whether a stable hydrogen-passivated cluster possessing a clean gap can be fabricated. To shed light on this situation, we have considered the hydrogen passivation of the unrelaxed cluster $Si_{200}$. The unrelaxed $Si_{200}$ cluster is constructed in the following way: The Si atoms are placed on the regular tetrahedral sites. But on the last incomplete shell, the Si atoms are distributed on the tetrahedral site in a random manner. Hence a cluster constructed in this way will have undistorted local bonding configuration but not an overall symmetry. For the particular cluster considered, there are 158 dangling bonds associated with this unrelaxed configuration. We passivate these dangling bonds with hydrogen atoms and calculate the DOS of both unrelaxed $Si_{200}H_{158}$ and relaxed $Si_{200}H_{158}$ clusters. In Fig. 10, the density of states for the unrelaxed $Si_{200}$, unrelaxed $Si_{200}H_{158}$, and relaxed $Si_{200}H_{158}$ are shown. It can be seen that the unrelaxed $Si_{200}$ cluster, as in the case of a cluster with filled shells (e.g., $Si_{83}$), possesses a clean gap and the lower edge of this gap does not begin at HOMO. The unrelaxed but hydrogen passivated $Si_{200}H_{158}$ has a much wider gap than that of the unrelaxed $Si_{200}$ and this gap begins at HOMO. Finally, there is hardly any change in the width of the gap between the relaxed and unrelaxed $Si_{200}H_{158}$ clusters. We find that results for a cluster with an incomplete shell are analogous to those for a cluster with filled shells (e.g., $Si_{83}$).

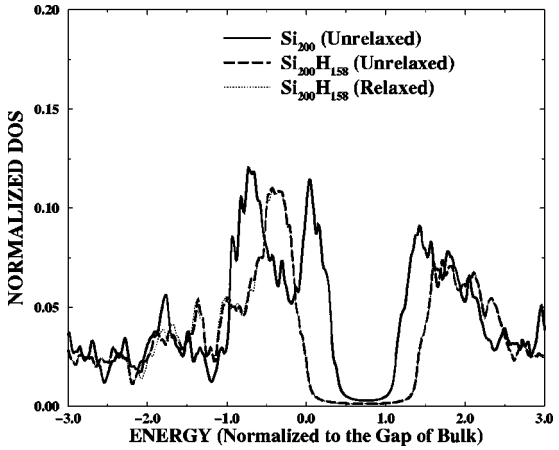


FIG. 10. A comparison of the normalized electronic density of states of unrelaxed $Si_{200}$, unrelaxed $Si_{200}H_{158}$, and relaxed $Si_{200}H_{158}$.

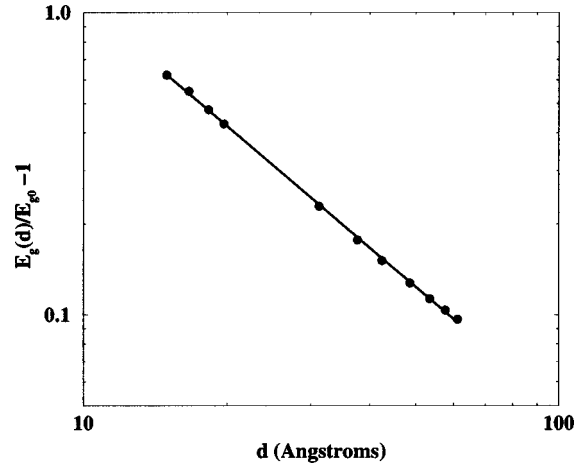


FIG. 11. The energy gap of the hydrogen-passivated silicon cluster as a function of the size of the cluster.

The fact that the unrelaxed $Si_{200}$ possesses a clean gap indicates that the existence of the gap only depends on the local bonding configuration rather than the overall symmetry.

The findings shown in Fig. 10 indicate that one may produce a cluster with a well-defined clean gap by passivating an unrelaxed cluster with hydrogen or other appropriate atomic species regardless of the size of the cluster (i.e., number of atoms in the cluster). But, the passivation must be completed before the cluster has the time or the opportunity to relax, or the passivation is carried out through a combined process of annealing and passivation. Detailed information on the time scales in the above-mentioned processes requires a study of the kinetics of hydrogen passivation. In the absence of such detailed calculations, one can gather evidence from experiments and make some general remarks. It is known that hydrogen passivation of the Si(100) surface at 295 K leads to the formation of $1\times1$ surface.[34] Carrying over this analogy to the cluster case, one may speculate that it should be possible to hydrogen passivate an unrelaxed silicon cluster around room temperature.

## V. THE SIZE DEPENDENCE OF THE GAP FOR A GENERAL CLUSTER

In this section, we study the size dependence of the energy gap for relaxed, hydrogen-passivated Si clusters of arbitrary sizes with no bond distortion. Relaxation ensures that the cluster is in a stable equilibrium configuration. Since there is no longer an overall symmetry associated with such a general cluster, no symmetry-based consideration can be used to reduce the computing effort of solving the eigenvalue problem and/or determining the DOS (see, for example, Ref. 6). For such a general cluster with a size beyond 1000 atoms, the calculation of DOS becomes computationally excessive. While the method of RSGF is efficient and convenient to calculate the DOS for large systems with no or reduced symmetry,[26] it is not a convenient tool to determine the energy gap, particularly if one wants to achieve good accuracy for the gap. This is because an accurate determination of the gap requires an accurate calculation of the energies of both the HOMO as well as the LUMO. To do this with the method of RSGF, one has to calculate $\mathrm{Im}\,G(E+i\epsilon)$ in the regions of the band edges at an energy interval sufficiently small compared to $\Delta E_{\mathrm{av}}$, the average separation between consecutive eigenvalues. In addition, one has to calculate these quantities for a series of decreasing $\epsilon$ (smaller than $\Delta E_{\mathrm{av}}$) to assure the convergence of the result. The whole process, while doable, can be time consuming. Therefore, we have developed a scheme, as described in the Appendix, that directly computes the eigenvalues corresponding to HOMO and LUMO without having to obtain the entire eigenvalue spectrum. This method is ideally suited for situations where selected eigenvalues of a large matrix are required.

Using the method outlined in the Appendix, we have carried out a series of very accurate calculations of the energy gap for relaxed, hydrogen-passivated $Si_NH_M$ clusters of various sizes with no bond distortion. In particular, we have performed the energy gap calculation for the following sets of $N$ (number of Si atoms) and $M$ (number of H atoms), respectively: $(N,M)=(200,158),(800,372),(1400,518),(2000,636),(3000,828),(4000,1012),(5000,1276)$, and $(6000,1354)$. Denoting the energy gap of a cluster of diameter $d=3.3685N^{1/3}$ (in Å , see Ref. 35) as $E_g(d)$ and that of the bulk as $E_{g0}$ (both in eV), we have shown in Fig. 11, the log–log plot of $[E_g(d)/E_{g0}]-1$ as a function of $d$. We find that the energy gap as a function of diameter of the cluster can be fitted to an equation of the form

$$\frac{E_g(d)}{E_{g0}}-1=\frac{24.98}{d^{1.364}}, \tag{8}$$

indicating a power law behavior for the effect of the quantum confinement for a general Si cluster as a function of the cluster size. This result is similar to the one reported previously for the size dependence of the energy gap of the hydrogen-passivated Si clusters with complete shells,[35] namely,

$$\frac{E_g(d)}{E_{g0}}-1=\frac{88.34/E_{g0}}{d^{1.37}}. \tag{9}$$

Since the energy gap of bulk Si obtained with the NOTB Hamiltonian[24] used in this calculation has a value $E_{g0}=3.16$ eV, one can rewrite Eq. (9) to yield

$$\frac{E_g(d)}{E_{g0}}-1=\frac{27.96}{d^{1.37}}. \tag{10}$$

A comparison of Eqs. (8) and (10) indicates that for the relaxed, hydrogen-passivated Si nanocluster of arbitrary size and with no bond distortions, the size dependence of its energy gap follows almost an identical pattern as that for the hydrogen-passivated clusters with full symmetry and no bond distortions. This suggests that the overall symmetry is not a relevant factor in the size dependence of the energy gap of a cluster.

## VI. SUMMARY

We have identified the factors responsible for the stability and the origin of a clean energy gap of a silicon nanocluster. We find that the existence of local configurations with no bond distortion is the key to the emergence of an energy gap. This is demonstrated by considering unrelaxed clusters with no bond distortion for which an energy gap exists no matter whether we consider a cluster with full shell (i.e., overall symmetry) or a cluster with an incomplete shell. However, the energy gap of unrelaxed clusters does not start at HOMO. This is due to the presence of dangling bond states. We have shown that a silicon cluster with no bond distortion and with its dangling bonds completely passivated will possess a wide and clean energy gap. Although the relaxation process can also eliminate dangling bond states, we find that this process introduces impurity states in the gap associated with the bond distortion of surface atoms in the cluster. These impurity modes cannot be eliminated by further saturation of remnant dangling bonds with hydrogen. In conclusion, we find that the relaxed hydrogen-passivated silicon nanoclusters with no bond distortions have the cleanest energy gap and the most stable structure among the different cases studied in this article.

## ACKNOWLEDGMENTS

This work was supported by the NSF (Grant No. DMR-9802274) and the DOE (Grant No. DE-FG02-00ER45832).

## APPENDIX: A METHOD FOR CALCULATING THE SELECTED EIGENVALUES OF A LARGE MATRIX

This method for finding selected eigenvalues is built around the ideas of real-space Green's function[26] and the conjugate gradient method.[36]

Starting from a generalized eigenvalue equation given in Eq. (1), it can be shown easily that

$$G(E)SC_\lambda=\frac{1}{E-E_\lambda}C_\lambda, \tag{A1}$$

where $G(E)$ is the (generalized) Green's function defined by

$$G(E)=(ES-H)^{-1}. \tag{A2}$$

To determine a particular eigenvalue $E_{\lambda_0}$ of the matrix, we start with an arbitrary vector $C^{(0)}$ and then generate a series of vectors $C^{(n)}$ iteratively according to the equation

$$C^{(n)}=G(E)SC^{(n-1)}, \quad n=1,2,3,\cdots. \tag{A3}$$

By writing $C^{(0)}$ as a linear combination of eigenvectors $C_\lambda$, namely,

$$C^{(0)}=\sum_\lambda a_\lambda C_\lambda, \tag{A4}$$

it can be seen that

$$C^{(n)}=\sum_\lambda \frac{a_\lambda}{(E-E_\lambda)^n}C_\lambda. \tag{A5}$$

By choosing the value of $E$ to lie close to $E_{\lambda_0}$, a particular eigenvalue among all the eigenvalues of the matrix, it is possible to determine the value of $E_{\lambda_0}$ as accurately as one desires using the formula

$$E_{\lambda_0}=E-\lim_{n\to\infty}\frac{C^{(0)T}SC^{(n)}}{C^{(0)T}SC^{(n+1)}}. \tag{A6}$$

In principle, this method can be used to calculate any particular eigenvalue and its corresponding eigenvector for large systems if we take advantage of the RSGF[26] method for calculating $G(E)$. However, the procedure as outlined in Eqs. (A3) and (A6) requires the repeated multiplication of the matrix $G(E)$ on a vector. Since $G(E)$ is not a sparse matrix even when $H$ and $S$ are sparse matrices, the computational effort and computing resources needed for calculating the series of $C^{(n)}$ can become excessive when the system size under consideration is very large and the computing resources are limited to desktop workstations. Therefore, we have developed an alternative scheme that takes advantage of the sparseness of the matrices $H$ and $S$. In this scheme, we avoid the step involving the calculation of the Green's function. We invert the expression given in Eq. (A3) such that we can now determine $C^{(n)}$ from $C^{(n-1)}$ by solving the equation

$$(ES-H)C^{(n)}=SC^{(n-1)}, \tag{A7}$$

using the conjugate gradient method as outlined in Ref. 36. Once consecutive $C^{(n)}$s are determined, they can be substituted into Eq. (A6) to determine $E_{\lambda_0}$.

In implementing the conjugate gradient scheme, we start from an arbitrary vector $C_0^{(n)}$ and choose $A_0$ and $B_0$ such that

$$A_0=B_0=SC^{(n-1)}-(ES-H)C_0^{(n)} \tag{A8}$$

from which a sequence of vectors $A_i$, $B_i$, and $C_i^{(n)}$ ($n=1,2,3,\ldots$) can be generated by using the following set of formulas:

$$A_{i+1}=A_i-\alpha_i(ES-H)B_i, \tag{A9}$$

$$B_{i+1}=A_{i+1}+\beta_i B_i, \tag{A10}$$

$$C_{i+1}^{(n)}=C_i^{(n)}+\alpha_i B_i, \tag{A11}$$

where

$$\alpha_i = \frac{A_i^T A_i}{B_i^T (ES-H) B_i}, \tag{A12}$$

$$\beta_i = \frac{A_{i+1}^T A_{i+1}}{A_i^T A_i}. \tag{A13}$$

The iterative procedure can be terminated when $A_m \to 0$ and when this condition is satisfied, it can be shown that $C_m^{(n)} \to C^{(n)}$. This is proved below. Using Eqs. (A8), (A9) and (A11), it can be shown that

$$\begin{aligned}(ES-H)C_m^{(n)} &= (ES-H)C_m^{(n)} + A_m \\ &= (ES-H)C_{m-1}^{(n)} + A_{m-1} \\ &= \cdots \\ &= (ES-H)C_0^{(n)} + A_0 \\ &= SC^{(n-1)}.\end{aligned} \tag{A14}$$

Using $SC^{n-1}$ as given in Eq. (A7) in the above equation, it can be seen that indeed

$$C_m^{(n)} \to C^{(n)} \tag{A15}$$

when $A_m \to 0$.

The main computational burden in calculating the $C^{(n)}$ and hence the eigenvalue as given by Eq. (A6) is now shifted to the calculation $(ES-H)B_i$, which involves the multiplication of a matrix and a vector. However, this matrix is sparse because both $S$ and $H$ for most systems of interest are sparse in the real-space representation. Because of this reason, the computational effort in evaluating specific eigenvalues becomes quite tractable even when the dimension of the system matrix is large. In the present work, the largest matrix that we have considered has the dimension $25\,354 \times 25\,354$ and the computation was done on a HP J-282 (180 MHz) with 256 MB RAM.

[1] T. Canham, Appl. Phys. Lett. **57**, 1046 (1990).
[2] A. Halimaoui, C. Oules, G. Bomchil, A. Bseiesy, F. Gaspard, R. Herino, M. Ligeon, and F. Muller, Appl. Phys. Lett. **59**, 304 (1991).
[3] Y. H. Xie, W. L. Wilson, F. M. Ross, J. A. Mucha, E. A. Fitzgerald, J. M. Macaulay, and T. D. Harris, J. Appl. Phys. **71**, 2403 (1992).
[4] *Light Emission from Silicon*, edited by S. S. Iyer, R. T. Collins, and L. T. Canham, MRS Symposia Proceedings No. 256 (Materials Research Society, Pittsburgh, 1992).
[5] K. A. Littau, P. J. Szajowski, A. J. Muller, A. R. Kortan, and L. E. Brus, J. Phys. Chem. **97**, 1224 (1993).
[6] S. Y. Ren and J. D. Dow, Phys. Rev. B **45**, 6492 (1992).
[7] J. P. Prost, C. Delerue, and G. Allan, Appl. Phys. Lett. **61**, 1948 (1992).
[8] B. Delley and E. F. Steigmeier, Phys. Rev. B **47**, 1397 (1993).
[9] M. Hirao, T. Uda, and Y. Murayama, Mater. Res. Soc. Symp. Proc., **283** , 425 (1993)
[10] M. Hirao and T. Uda, Surf. Sci. **306**, 87 (1994).
[11] T. Uda and M. Hirao, J. Phys. Soc. Jpn. **63**, 97 (1994).
[12] L. W. Wang and A. Zunger, J. Phys. Chem. **98**, 2158 (1994); L. W. Wang, Phys. Rev. B **49**, 10154 (1994).
[13] F. Kozlowski and W. Lang, J. Appl. Phys. **72**, 5401 (1992).
[14] G. D. Sanders and Y.-C. Chang, Phys. Rev. B **45**, 9202 (1992).
[15] C. Delerue, G. Allen, and M. Lannoo, Phys. Rev. B **48**, 11024 (1993).
[16] M. S. Hybertsen, Phys. Rev. Lett. **72**, 1514 (1994).
[17] A. J. Reed, R. J. Needs, K. J. Nash, L. T. Canham, P. D. J. Calcott, and A. Oteish, Phys. Rev. Lett. **69**, 1232 (1992).
[18] M. S. Brandt, H. D. Fuchs, M. Stutzmann, J. Weber, and M. Cardona, Solid State Commun. **81**, 307 (1992).
[19] F. Koch, V. Petrova-Koch, T. Muschik, A. Nikolov, and V. Gavrilenko, Mater. Res. Soc. Symp. Proc. **283**, 197 (1992).
[20] S. M. Prokes, J. Appl. Phys. **73**, 407 (1993).
[21] M. H. Nayfeh, N. Barry, J. Therrien, O. Akcakir, E. Gratton, and G. Belomoin, Appl. Phys. Lett. **78**, 1131 (2001).
[22] G. Allan, C. Delerue, and M. Lannoo, Phys. Rev. Lett. **76**, 2961 (1996).
[23] M. H. Nayfeh, N. Rigakis, and Z. Yamani, Phys. Rev. B **56**, 2079 (1997).
[24] M. Menon and K. R. Subbaswamy, Phys. Rev. B **55**, 9231 (1997).
[25] C. S. Jayanthi, S. Y. Wu, J. A. Cocks, N. S. Luo, Z. L. Xie, M. Menon, and G. Yang, Phys. Rev. B **57**, 3799 (1998).
[26] S. Y. Wu and C. S. Jayanthi, Int. J. Mod. Phys. B **9**, 1869 (1995).
[27] E. Kaxiras, Phys. Rev. B **56**, 13455 (1997).
[28] D. R. Alfonso, S. Y. Wu, C. S. Jayanthi, and E. Kaxiras, Phys. Rev. B **59**, 7745 (1999).
[29] S. Liu, C. S. Jayanthi, S. Y. Wu, X. Qin, Z. Zhang, and M. G. Lagally, Phys. Rev. B **61** 4421 (2000).
[30] K. Takayanagi, Y. Tanishiro, N. Takahashi, and S. Takahashi, J. Vac. Sci. Technol. A **3**, 1502 (1985).
[31] S. Lanzavecchia and L. Colombo, Europhys. Lett. **36**, 295 (1996).
[32] M. V. Ramana Murty and H. A. Atwater, Phys. Rev. B **51**, 4889 (1995).
[33] A. A. Seraphin, S. T. Ngiam, and K. D. Kolenbrander, J. Appl. Phys. **80**, 6429 (1996).
[34] M. Terashi, J. Kuge, M. Shinohara, D. Shoji, and M. Niwano, Appl. Surf. Sci. **130**, 260 (1995).
[35] A. Zunger and L.-W. Wang, Appl. Surf. Sci. **102**, 350 (1996).
[36] W. H. Press, S. A. Teukolsky, W. T. Vetterling, and B. P. Flannery, *Numerical Recipes* (Cambridge University Press, Cambridge, 1986).